

# Preparation of SiO<sub>2</sub>/ZrO<sub>2</sub> Ceramic Nanocomposite Coating on Aluminum Alloys as Metallic Part of the Photovoltaic Cells and Study its Corrosion Behavior

Seyyed Behnam Abdollahi Boraei<sup>a</sup>, Mehdi Esmaili Bidhendi<sup>b\*</sup>, Daryoush Afzali<sup>c</sup>

<sup>a</sup> Department of Life science Engineering, Faculty of New Sciences and Technologies, University of Tehran, Tehran, Iran

<sup>b</sup> Graduate Faculty of Environment, University of Tehran, Iran

<sup>c</sup> Department of Chemistry, Graduate University of Advanced Technology, Kerman, Iran

Received: 21 November 2016 /Accepted: 16 April 2017

## Abstract

Nowadays due to water shortage, the use of air humidity as the sustainable solution has been considered by cities located in coastal zones; especially in warm and humid climate. However, the use of air humidity also has its own problems such as corrosion of metal parts in photovoltaic cells that used for energy supplying and they are often made of Aluminum alloy. Therefore different methods such as coating have been considered by the user of photovoltaic cells in corrosive conditions in order to reduce corrosion. So in this study, SiO<sub>2</sub>- ZrO<sub>2</sub> ceramic nanocomposite coatings were put on AA2024-T4 Aluminum alloy by Sol-Gel method and dip-coating technique. The films with different compositions have been prepared and morphology and functional groups of samples have been specified by Scanning Electron Microscopy (SEM) and Fourier Transform Infrared Spectroscopy (FTIR). The corrosion behavior of the coatings was evaluated by polarization and electrochemical impedance spectroscopy (EIS) measurement in 3.5 % NaCl. The results base on polarization and EIS showed that SiO<sub>2</sub>-ZrO<sub>2</sub> ceramic nanocomposite coatings improved corrosion resistance properties of Aluminum alloy and film with 0.25ml Zirconium alkoxide shows the best corrosion resistance.

**Keywords:** Sol-Gel, Nanocomposite, Corrosion, Aluminum Alloy, Photovoltaic Cell

## Introduction

In the recent decades, the notable increase in population, excessive use of water and climate changes have been caused water scarcity, extensive reduction in capacity of raw water resources and the occurrence of new pollutants; led to the reduction in quality of raw water (Jabran et al. 2017; Noman et al. 2017 and Saud et al. 2016).

Therefore in recent years and in response to growing demand for drinking water and according to necessity of sustainable development especially in developing countries with arid and semi-arid climate, use of non-conventional water resources is considered (Shen et al. 2005; Zhang et al. 2003; Davtalab et al. 2013 and Wang et al. 2017). In relation to achievement this goal, different water resources such as municipal wastewater, artificial rain and snow have been

---

\* Corresponding author E-mail: esmaeilb@ut.ac.ir

used globally. However, in some regions and on the basis of local conditions and limitations, other non-conventional resources also have been used; one of them is air humidity.

Air humidity is the most common of non-conventional water resources which according to statistically researches its amount is estimated 14000 km<sup>3</sup>, in contrast 1200 km<sup>3</sup> for freshwater (Hamed, 2000 and Gandhidasan et al. 2010). This source can be harvest in many parts of the earth specific coastal zones. The coastal zones especially with warm and humid climate do not receive enough precipitation at any period during the year, are the main area for harvesting water from air humidity. Because of two important reasons; first reason is the lack of raw conventional water resources, aridity and scarcity of water due to small amount of precipitation in these areas and second reason is surrounding these areas by the fog often due to whole of the year and huge amount of humidity in the air; harvesting water from air humidity is the important and sustainable local non-conventional water resource in coastal zones (Davtalab et al. 2013 and Girja, 2006). In this regard different country such as Kingdom of Saudi Arabia, Peru and Chile and also international research centers, have started especial programs and projects for harvesting water from air humidity (Davtalab et al. 2013 and Girja, 2006).

Harvesting water from air humidity is on the basis of dense thermodynamic processes and being air humidity in the stage of saturation and density are the specific characteristics that have the important role for water harvesting; in fact for water harvesting, with relative air humidity above 68-90%, the conditions are appropriate, and fog will be formed in humidity above 98% (Esfandyarnejad et al. 2009). For harvesting water from air humidity, based on condensation technology, several systems with different capacities and structures are designed and used; but all of them need a power supply section for supplying energy continuously and compatible with sustainable development's goals. Hence photovoltaic cells that convert solar energy to electricity, normally used for supplying energy for harvesting water from air humidity; especially in areas with more sunny days. However, the use of photovoltaic cells, according to the materials of their components and environmental conditions, is associated with own problems. Photovoltaic cells are made of different metallic and non-metallic parts; more metallic parts of the photovoltaic cells are made of aluminum alloy, which these parts are vulnerable to the corrosive conditions in the environment. One of the most corrosive conditions that effect on the metal parts of solar cells appears in coastal zones with warm and humid climate; the cause of existing natural phenomenon, the sea salt spray that it consists of organic and inorganic salts such as Sodium Chloride (NaCl) as the corrosive natural agent.

According to the above, we must use new technology for reduction corrosion on the metallic parts in photovoltaic cell's structures. In regard to this matter, various methods have been identified to reduce corrosion; nanocomposites because of their especial characteristics such as high resistance to wear and corrosion, hot oxidation resistance, dispersion hardening and self-lubrication are one of the most effective methods (Kimura and Masumoto, 1984; Ma et al. 2007; Zou et al. 2009; Yu et al. 2008 and Wang et al. 2010). Hence, in this research, an attempt is made to promote corrosion resistance of AA-2024-T4 Aluminum alloy with the use of SiO<sub>2</sub>/ZrO<sub>2</sub> nanocomposite coating by sol-gel method (it is widely used for the preparation of coating on metal substrates) and assessment the structure of coating material, its electrochemical behavior and properties against the corrosive condition.

## **Materials and methods**

### *Materials*

AA2024-T4 Aluminum alloy samples used in this research were of industrial grade purchased from Tehran central Aluminum market. All chemicals and reagents for the sols used in this

research were of analytical grade purchased from Sigma-Aldrich Company; also doubly distilled deionized water was used throughout for preparing all solutions.

#### *Sol and coating preparation*

Tetraethoxysilane (TEOS) and Zirconium (IV) Isopropoxide were used as inorganic metal alkoxide precursors; also Ethanol (96%) was used as the solvent. In the synthesis of the solutions, TEOS and Ethanol (EtOH) were mixed for 2 hours at room temperature before addition of Zirconium (IV) Isopropoxide. Then Zirconium (IV) Isopropoxide diluted with Ethanol and the mixture ultrasonically agitated for 1 hour at room temperature. To control the rate of hybridization, simultaneous ethyl Acetoacetat (EAcAc) was added next; then the mixture ultrasonically agitated for 1 hour at room temperature. The concentrated HNO<sub>3</sub> solution was used to control pH, till pH became 2. The prepared sol was agitated for 1 hour at room temperature and then it was dried at 90 °C for 1 hour. Finally, to study the effect of Zirconium (IV) Isopropoxide on microstructure and corrosion behavior, 0.15, 0.20, 0.25 and 0.30 ml of Zirconium (IV) Isopropoxide, was added to the sol of TEOS and Ethanol (EtOH).

#### *Surface preparation and coating*

AA2024-T4 Aluminum alloy samples were mechanically polished using 180 to 1000 grit papers sequentially. Then the samples were rinsed in Acetone and Ethanol for 15 and 10 minutes respectively by an ultrasonic cleaner in order to degrease and clean the surfaces. Then cleaned samples were coated by the dip-coating method; the withdrawal speed was 4 cm/min.

#### *Electrochemical tests*

Corrosion behavior of coatings was measured by using electrochemical EIS techniques in 3.5% NaCl solution with a Potentiostat/Galvanostat GSTAT 302N instrument. Samples were immersed in the testing solution for 2 hours before each test. Scan rate 100 mV/s was used for potentiodynamic tests. EIS tests were carried out at the frequency range of 10<sup>-2</sup>-10<sup>2</sup> Hz. Each test repeated for three times to confirm the repeatability of the results of the experiment.

#### *Characterization technique*

##### *Scanning electron microscopy*

Scanning electron microscopy (SEM) measurements were used on the surface of coated substrates to characterize the surface morphology by an EM3200 Chinese instrument. Secondary and backscattered electron images were collected at 2500 and 15000 magnification at 26 kV.

##### *FTIR measurements*

FTIR is a useful method for identifying chemical bonds and functional groups of substances. FTIR measurements were carried out in the range from 600 to 4000 cm<sup>-1</sup>. This analysis provides a different wavelength for each substance. All spectra were obtained at an incident angle of 45° normal to the surface of the specimen, with a spectral resolution of 4 cm<sup>-1</sup>. For each measurement, 64 scans were collected.

## **Results and discussion**

### *FTIR results*

Figure 1 shows the FTIR spectra of Silica-Zirconia nanocomposite coating with 0.25ml Zr alkoxide. The result bonds are include the hydroxide group bending between  $2600-3700\text{ cm}^{-1}$ , the C-C band at  $1636\text{ cm}^{-1}$ , the C-O band at  $1067\text{ cm}^{-1}$  and the Zr-O and Si-O metallic bands at under  $1000\text{ cm}^{-1}$  peaks (Zhong et al. 2009; Malekmohammadi et al. 2011 and Ruhi et al. 2008).

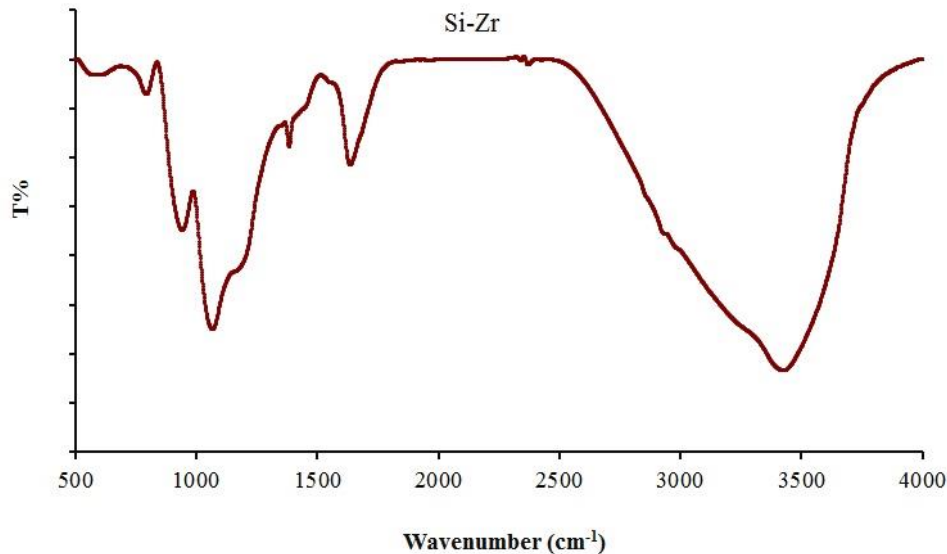


**Figure 1.** FTIR spectra Si/Zr nanocomposite coating that heat treated at  $450\text{ }^{\circ}\text{C}$

### *Electrochemical results*

#### *Potentiodynamic polarization*

The potentiodynamic curves of uncoated and Silica-Zirconia nanocomposite coatings in 3.5% NaCl solution are shown in figure 2. Effect of Silica-Zirconia nanocomposite coatings is conspicuous in potentiodynamic curves of coated samples which shift to the left side and to more noble potentials by increasing the Silica-Zirconia concentration till 0.25ml Zr alkoxide. These curves illustrate the benefits of Silica-Zirconia nanocomposite coating to make the surface more corrosion resistant.

Corrosion current density ( $i_{\text{corr}}$ ), corrosion rate (CR), corrosion potential ( $E_{\text{corr}}$ ) of the uncoated and Silica-Zirconia nanocomposite coating were tabulated in table 1. Corrosion inhibition properties of Silica-Zirconia nanocomposite coating might be the main reason for the increase of corrosion resistance of the AA2024-T4 Aluminum alloy.

#### *Electrochemical impedance spectroscopy*

In this study for quantitative investigation of the effect of Silica-Zirconia nanocomposite coatings on electrochemical properties of the surface of AA2024-T4 Aluminum alloy, EIS was used. Nyquist curves of uncoated and Silica-Zirconia nanocomposite coatings were presented in figure 3.

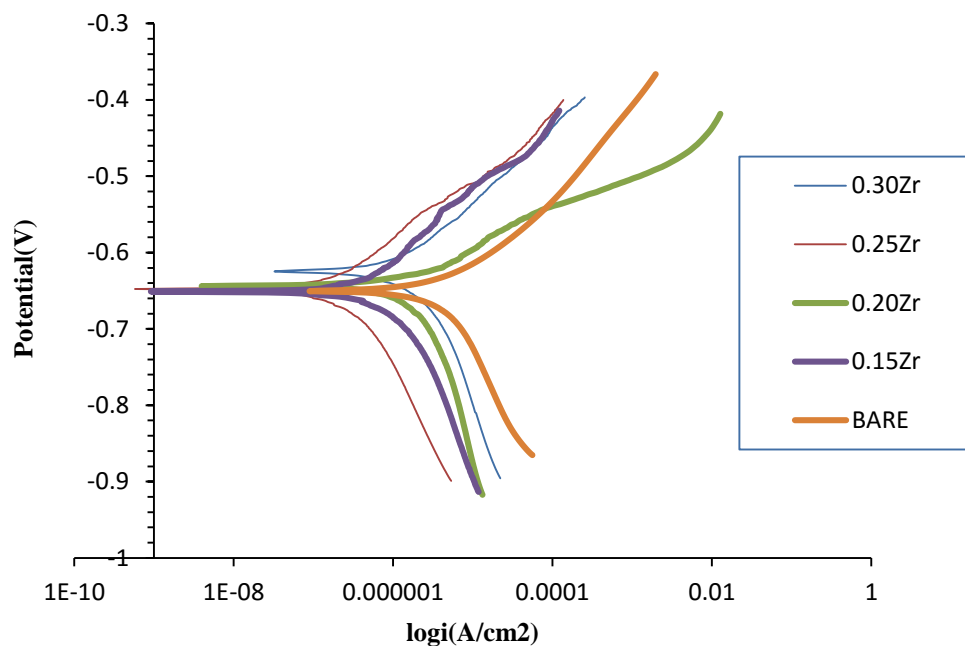


**Figure 2.** Potentiodynamic polarization curves of bare, coating and nanocomposite coating with 0.15, 0.20, 0.25, 0.3 Zr.

**Table 1.** Electrochemical parameters of uncoated and Silica-Zirconia nanocomposite coatings

Electrochemical parameters	Bare	Si-0.15Zr	Si-0.20Zr	Si-0.25Zr	Si-0.30Zr
$i_{corr}$ (nA cm <sup>-2</sup> )	829.43	179.49	121.64	14.63	336.31
$E_{corr}$ (mV)	-752.34	-650.98	-643.83	-647.79	-624.35
$\beta_a$ (mV/decade)	6.43	26.60	48.45	10.06	28.87
$\beta_c$ (mV/decade)	16.77	38.34	62.03	9.79	25.10

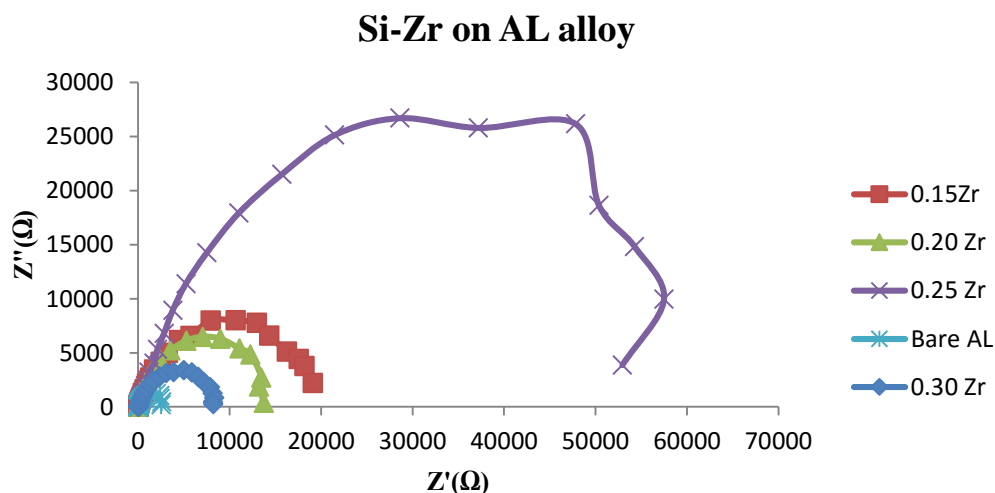


**Figure 3.** Nyquist plots of bare sample, Si coating and Si/Zr nanocomposite coating with different amounts of Zr.

It can be found from these curves that in high frequency region ( $10^{-2}$ - $10^2$  Hz), a layer is formed on the surface of AA2024-T4 Aluminum alloy. High frequency region in impedance spectroscopy describes the behavior of the coating and the aforementioned results indicate that the coating has been formed on the surface of AA2024-T4 Aluminum alloy. EIS measurements that are presented in table 2, confirmed the conclusions drawn out of the SEM micrographs in figure 4 and figure 5 about the formation of Silica-Zirconia nanocomposite coatings areas on the surface of the AA2024-T4 Aluminum alloy.

**Table 2.** Important parameters of EIS measurement

	$R_s$ ( $\Omega$ )	Q	n	L	$R_L$ ( $\Omega$ )	$R_{ct}$ ( $\Omega$ )
BARE	13.39	2.358E-5	0.79	47350	8329	548.7
Si-0.15Zr	18.67	1.554E-5	0.79	5960	3599	18630
Si-0.20Zr	9.052	1.447E-5	0.88	39140	6929	7997
Si-0.25Zr	18.57	2.736E-5	0.75	75870	25530	64110
Si-0.30Zr	6.419	7.042E-6	0.91	47350	3907	31930

As it can be seen in this table due to corrosive-inhibitive properties of Silica-Zirconia, the electrical resistance of Silica-Zirconia sol-gel film is higher than the uncoated sample and consequently, their corrosion resistance is greater. Furthermore, it can be confirmed that there is a critical Silica-Zirconia concentration for beneficial effects of Silica-Zirconia on corrosion resistance over which increasing the Silica-Zirconia concentration decreased resistant of the sol-gel film. The addition of Silica-Zirconia more than the optimal concentration can be attributed to the high coefficient of expansion of Silica-Zirconia oxide which strengthens the probability of cracking concomitant with Silica-Zirconia content increase. It can be deduced from EIS studies which represented in table 2, that  $n$  parameter which is an indicator of surface roughness decreased. An increase in a number of cracks and defects in the sol-gel film is the main responsible for this negative effect. It can be related to the creation of Silica-Zirconia islands which cause increasing of surface roughness. Also, it can be found that increasing the amount of Silica-Zirconia from 0.25 ml will lead to an increase of the roughness value. This can be related to increasing of Silica-Zirconia islands by increasing the amount of Silica-Zirconia which was observed also in SEM and EIS studies. From table 2 it can be found that capacitance of Silica-Zirconia nanocomposite coatings is higher than uncoated samples.

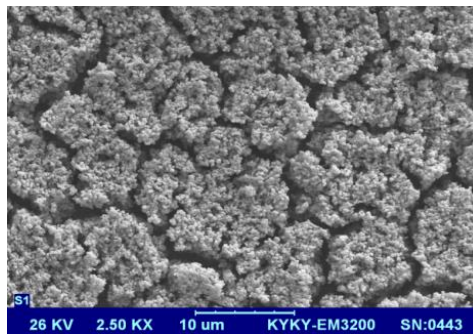


**Figure 4.** Nanocomposite ceramic coating with heat treatment at 450 ° C, at 2500 times magnifications

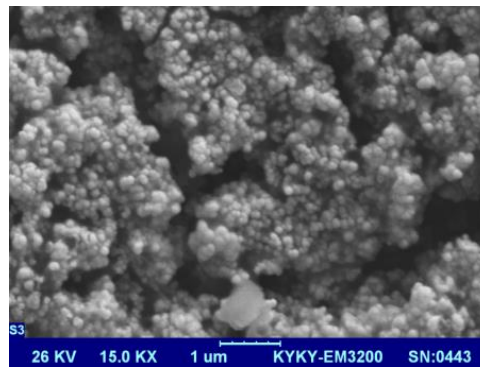


**Figure 5.** Nanocomposite ceramic coating with heat treatment at 450°C, at 15000 times magnifications

To measure the electrochemical properties of the uncoated and Silica-Zirconia nanocomposite coatings, equivalent circuits were selected which best describes the corrosion behavior of the films. The equivalent circuit for Silica-Zirconia nanocomposite film is selected as in figure 6. This model parameters are as follows:  $R_s$  the solution resistance,  $R_{ct}$  the resistance of the sol-gel film,  $L$ : inductance,  $R_L$  the inductance resistance,  $Q$  the constant phase element of the sol-gel coating (Salarvand et al. 2017).

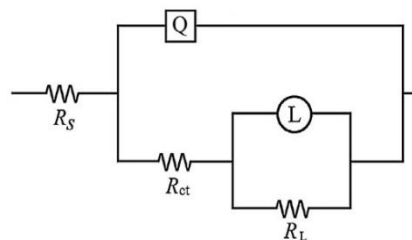


**Figure 6.** Simulated equivalent circuit

## Conclusion

The potentiodynamic polarization and EIS studies results indicated that the Zirconium nanoparticles significantly increased the corrosion performance of the coating. The advantages of incorporating these additives were evident from potentiodynamic and impedance measurements after an immersion time of 2 hours. Excellent corrosion resistance was obtained from Silica-Zirconia ceramic nanocomposite coatings on AA2024-T4 Aluminum alloy with 0.25ml Zr alkoxide; this amount of Zr caused smooth and crack free films. These corrosion resistance properties related to the nanostructure and phase of Silica-Zirconia ceramic nanocomposite oxide that all nanocomposite coatings showed better corrosion resistance in comparison with bare AA2024-T4 aluminum alloy. Finally and according to results of this research, use of Silica-Zirconia ceramic nanocomposite for preventing of photovoltaic cell's Aluminum parts corrosion in coastal zones with warm and humid climate is suggested.

## Acknowledgments

The authors acknowledge the financial and scientific support provided by the Kerman Graduate University of Advanced Technology and Graduate faculty of Environment at the University of Tehran.

## References

- Jabran, K., Riaz, M., Hussain, M., Nasim, W., Zaman, U., Fahad, S. and Chauhan, B. S. (2017). Water-saving technologies affect the grain characteristics and recovery of fine-grain rice cultivars in semi-arid environment. *Environmental Science and Pollution Research*, 1-11.

- Noman, A., Fahad, S., Aqeel, M., Ali, U., Anwar, S., Baloch, S. K., & Zainab, M. (2017). miRNAs: Major modulators for crop growth and development under abiotic stresses. *Biotechnology Letters*, 1-16.
- Saud, S., Yajun, C., Fahad, S., Hussain, S., Na, L., Xin, L. and Alhussien, S. A. A. F. E. (2016). Silicate application increases the photosynthesis and its associated metabolic activities in Kentucky bluegrass under drought stress and post-drought recovery. *Environmental Science and Pollution Research*. 23(17), 17647-17655.
- Shen, G.X., Chen, Y.C., Lin, L., Lin, C.J. and Scantlebury, D. (2005). Study on a hydrophobic nano-TiO<sub>2</sub> coating and its properties for corrosion protection of metals. *Electrochimica Acta*, 50(25-26), 5083–5089.
- Zhang, W., Liu, W. and Wang, C. (2003). Effects of solvents on the tribological behaviour of sol–gel Al<sub>2</sub>O<sub>3</sub> films. *Ceramics International*, 29(4), 427-434.
- Davtalab, R., Salamat, A. and Oji, R. (2013). Water harvesting from fog and air humidity in the warm and coastal regions in the south of Iran. *Irrigation and drainage*. 62(3), 281–288.
- Wang, J. H., Zhang, T. Y., Dao, G. H., Xu, X. Q., Wang, X. X. and Hu, H. Y. (2017). Microalgae-based advanced municipal wastewater treatment for reuse in water bodies. *Applied Microbiology and Biotechnology*. 101(7), 2659-2675.
- Hamed, A.M. (2000). Absorption–Regeneration Cycle for Production of Water from Air-theoretical Approach. *Renewable Energy*. 19(4), 625–635.
- Gandhidasan, P. and Abualhamayel, H. I. (2010). Investigation of humidity harvest as an alternative water source in the Kingdom of Saudi Arabia. *Water and Environment Journal*, 24 (4), 282-292.
- Girja, S. (2006). Dew Harvest. Foundation Books in association with Centre for Environment Education, New Delhi, India.
- Esfandyarnejad, A., Ahangar, R., Kaalian, R., Poorhatefi, M., Sangchooli, T. and Shafiei, R. (2009). Water harvesting from fog and air humidity in the coastal areas (Hormozgan case study). Research plan, Hormozgan regional water authority.
- Kimura, H. and Masumoto, T. (1984). Particle-dispersion hardening of an amorphous Ni<sub>78</sub>Si<sub>10</sub>B<sub>12</sub> composite. *Journal of Non-Crystalline Solids*, 61–62 , 835–839.
- Ma, S.L., Ma, D.Y., Guo, Y., Xu, B., Wu, G.Z., Xu, K.W. and Chu, P.K. (2007). Synthesis and characterization of super hard, self-lubricating Ti–Si–C–N nanocomposite coatings. *Acta Materialia*, 55(18), 6350–6355.
- Zou, B., Huang, C. and Chen, M. (2009). Study on the mechanical properties, microstructure and oxidation resistance of Si<sub>3</sub>N<sub>4</sub>/Si<sub>3</sub>N<sub>4</sub>W/Ti(C<sub>7</sub>N<sub>3</sub>) nanocomposites ceramic tool materials. *International Journal of Refractory Metals and Hard Materials*. 27(1), 52– 60.
- Yu, Q., Ma, X., Wang, M., Yu, C. and Bai, T. (2008). Influence of embedded particles on microstructure, corrosion resistance and thermal conductivity of CuO/SiO<sub>2</sub> and NiO/SiO<sub>2</sub> nanocomposite coatings. *Applied Surface Science*, 254(16), 5089–5094.
- Wang, L., Zhang, G., Wood, R.J.K., Wang, S.C. and Xue, Q. (2010). Fabrication of CrAlN nanocomposite films with high hardness and excellent anti-wear performance for gear application. *Surface and Coatings Technology*, 204(21-22), 3517–3524.
- Zhong, X., Li, Q., Chen, B., Wang, J. Hu, J. and Hu, W. (2009). Effect of sintering temperature on corrosion properties of sol–gel based Al<sub>2</sub>O<sub>3</sub> coatings on pre-treated AZ91D magnesium alloy. *Corrosion Science*, 51(12), 2950-2958.
- Malekmohammadi, F., Rouhaghdam, A. S. and Shahrabi, T. (2011). Effect of heat treatment on corrosion properties of mixed sol gel silica–titania (7–3) coating. *Journal of Non-Crystalline Solids*, 357(3), 1141-1146.
- Ruhi, G., Modi, O. P., Sinha, A. S. K. and Singh, I. B. (2008). Effect of sintering temperatures on corrosion and wear properties of sol–gel alumina coatings on surface pre-treated mild steel. *Corrosion Science*, 50(3), (2008) 639-649.
- Salarvand, Z., Amirnasr, M., Talebian, M., Raeissi, K., and Meghdadi, S. (2017). Enhanced corrosion resistance of mild steel in 1M HCl solution by trace amount of 2-phenyl-benzothiazole derivatives: Experimental, quantum chemical calculations and molecular dynamics (MD) simulation studies. *Corrosion Science*, 114, 133-145.

